# IAC-06- B3.4.01

# DEEP SPACE NETWORK AND LUNAR NETWORK COMMUNICATION COVERAGE OF THE MOON

**Charles H. Lee**
California State University Fullerton, USA
CharlesHLee@fullerton.edu

**Kar-Ming Cheung**
NASA Jet Propulsion Laboratory, USA
Kar-Ming.Cheung@jpl.nasa.gov

**ABSTRACT**

In this article, we describe the communication coverage analysis for the lunar network and the Earth ground stations. The first part of this article focuses on the direct communication coverage of the Moon from the Earth's ground stations. In particular, we assess the coverage performance of the Moon based on the existing Deep Space Network (DSN) antennas and the complimentary coverage of other potential stations at Hartebeesthoek, South Africa and at Santiago, Chile. We also address the coverage sensitivity based on different DSN antenna scenarios and their capability to provide single and redundant coverage of the Moon. The second part of this article focuses on the framework of the constrained optimization scheme to seek a stable constellation six relay satellites in two planes that not only can provide continuous communication coverage to any users on the Moon surface, but can also deliver data throughput in a highly efficient manner. Communication coverage of the lunar surface by both the existing and newly found lunar relay network will be compared. Other metrics such as the maximum and the number of communication gaps will also be addressed. The impacts of the relay lunar network on the DSN coverage of the Moon surface will also be investigated. We end the article with the discussions on the needs for the crosslink (orbiter-to-orbiter) communication capability and the means for mitigating lunar relay latency.

## Introduction

Communication links and coverage play an essential role in supporting human and robotic exploration of the Moon. An idealistic communication network with continuous linkage between Earth and the Moon will enable the missions to carry out mission at any opportunity, to go for any duration, to land at any location on the lunar surface, and to perform any scientific sorties. Our first goal in this paper is to understand the current coverage capabilities of the existing Deep Space Network (DSN) ground stations and to explore the enhanced coverage provided by different constellations of lunar relay satellites. The DSN sites of interest include the primary stations from Goldstone,

Canberra and Madrid. We also explore the added coverage from the Santiago, Chile and the Hartebeesthoek, South Africa sites. As expected and will be verified by our coverage analysis that direct line-of-sight communication with the existing DSN sites might not be sufficient to support missions to the polar regions, the near-side borders, and the far-side region of the moon. A constellation of relay lunar orbiters, when optimally found, will extend the communication linkage between the DSN stations and the entire lunar surface. In the second part of the paper we perform the constrained optimization study to seek a constellation of relay satellites that can meet a number of design criteria. First, each constellation must consist of six relay satellites, equally space in two perpendicular planes. These constellations are designed and optimized in a sense that their orbits are stable and require very little trajectory maintenance. We also impose the either the continuous visibility or the continuous coverage constraint on these constellations. By visibility, we mean the lunar surface is geometrically connecting to one of the satellites in the constellation with a direct line of sight (i.e. 0° elevation masks), whereas by coverage the line of sight must be 6° above the horizon. Evidently, the latter constraint would require the constellation to have higher altitudes so that the users on the lunar surface will experience no communication gaps with the relay satellites. At the same time the altitudes of these constellations must be as low as possible so that they can deliver telecom throughputs more efficiently.

The two optimized constellations we found are of circular frozen orbits that are phased and selected with the lowest altitudes to provide 100% visibility or 100% coverage for the entire lunar surface. It should be emphasized that our optimized constellations are inspired by the constellations proposed by [1]. For comparison purposes, we also analyze the communication coverage performance of those two constellations.

Future missions can benefit from our results in the sense that we can provide the information on the coverage, the worst case scenario gaps, and the frequency of the gaps. Such metrics are of great value to mission planning and science activities. We will end the paper with some discussions on the latency due to communication coverage, its mitigation, and the necessity of the crosslinks between relay orbiters.

## DSN Coverage of the Moon

In this section, we focus on the direct coverage of the lunar surface by the Deep Space Network (DSN). In our analysis, we assume the elevation mask angles for the DSN stations and the lunar surface locations are 20° and 6°, respectively. The simulation duration is one sidereal month (27.3217 days) with a four-minute time step and the starting epoch is 2010-169T04:00:19 (UTC). At each time instance, we determine whether a location at certain longitude and latitude on the Moon is connected to one of the DSN sites. Such temporal profile yields the percentage of coverage by the DSN. We calculated the coverage percentages for the entire lunar surface based on the 2-degree longitude and latitude resolution. We denote DSN3 to be the three primary DSN sites, which include Goldstone, Canberra, and Madrid. We also denote DSN4 to be a network of the previous three sites plus the Hartebeesthoek site. The lunar map of the coverage percentages based on DSN3 is displayed in Figure 1.

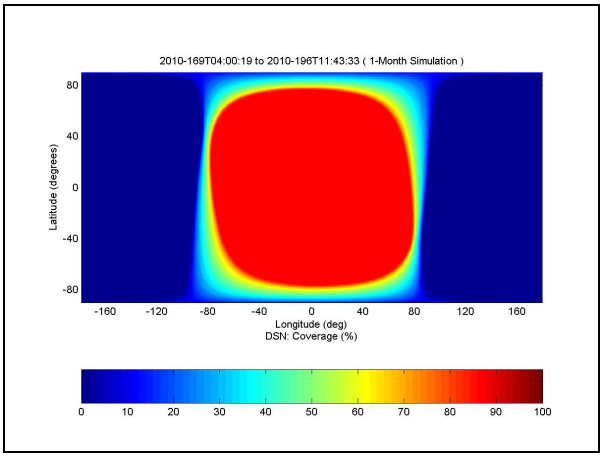


Fig. 1: Lunar map of the coverage percentage by DSN3. (6° lunar and 20° DSN elevation masks)

While the lunar map offers the global view of the coverage percentages, it is not always easy to read off the actual values. As an alternative visualization, we produce the latitude maps. Notice that in a latitude map, we extract and plot along each latitude the minimum, mean, and maximum values, so that should a mission be planned for that particular latitudinal band, the expected values can be found from these latitude maps. Three other pieces of information are

also provided in the latitude map: the area-weighted (A-W) mean is computed by averaging the value weighted by the cosine of the latitude, the absolute minimum, and the absolute maximum. A latitude map for the DSN coverage percentages derived from Figure 1 is provided in Figure 2.

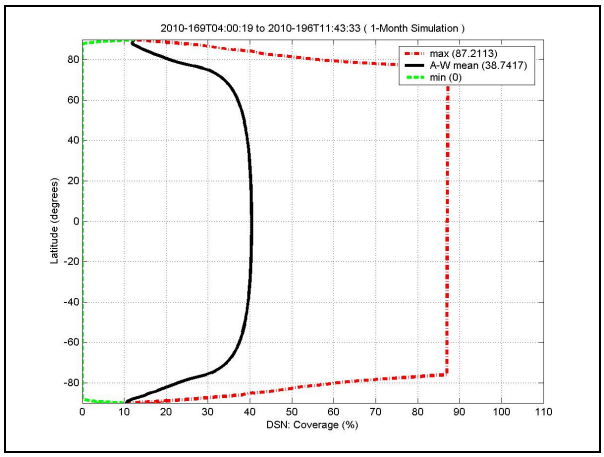


Fig. 2: Latitude map of the coverage percentage by DSN3. (6° lunar and 20° DSN elevation masks)

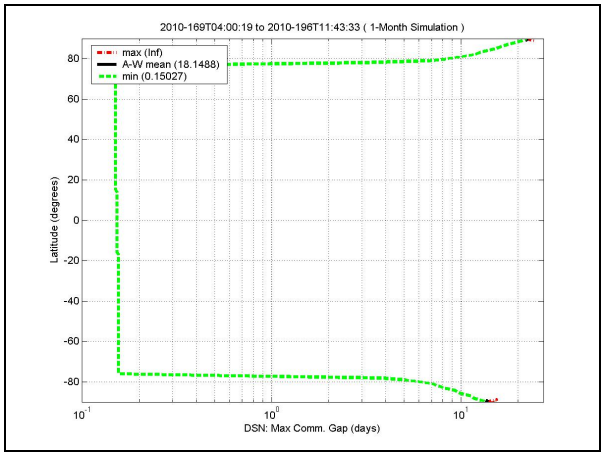


Fig. 3: Latitude map of the maximum communication gap between the Moon surface and DSN3. (6° lunar and 20° DSN elevation masks)

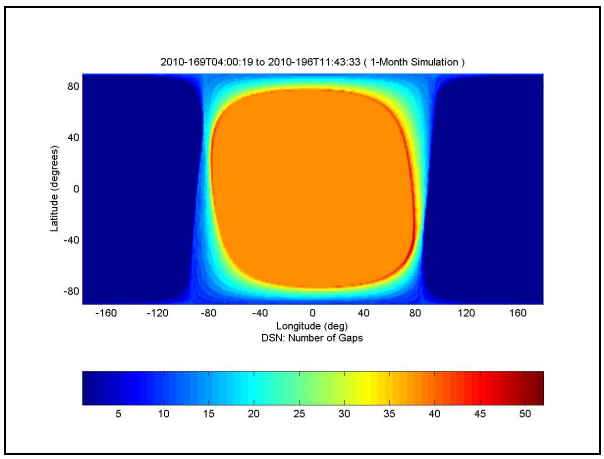


Fig. 4: Lunar map of the number of communication gaps between the Moon surface and DSN3. (6° lunar and 20° DSN elevation masks)

Other metrics of interest that can be extracted include the maximum communication gaps and the frequency of the gaps. These parameters are quite useful for mission planning, especially for manned missions. These metrics are shown in Figures 3 and 4.

Direct coverage of the Moon by the DSN stations can be summarized as follows. As expected, over 87 percent of the time DSN3 can cover the *near-side* of the Moon for all the latitudes between ±76°. Coverage in the northern region (near-side latitudes from 77° to 90°) is reduced to as low as 14%, whereas the southern coverage (near-side latitudes from -77° to -90°) could be as low as 10% of the time. Keep in mind that due to both the DSN and the lunar mask angle assumptions, the coverage percentages are not very high. For one lunar sidereal month simulation, the *near-side* region between the ±76° latitudes could experience 40-50 communication gaps, These gaps, caused by the 20° DSN elevation mask constraint, are mostly brief and the long ones could last as high as 3.6 hours. Note that these gaps are vanished, when the 0° DSN elevation mask constraint is imposed. While the poles experience fewer gaps (10 to 40), some of the gaps could be very long. For instance, for the gap in the northern region could be as long as 22 days and 13.6 days for the south.

In the previous analysis, we implemented with the baseline assumptions; That is, the DSN sites include Goldstone, Canberra and Madrid with the mask angles of 20° for DSN and 6° for the lunar surface. We extended the analysis to study the sensitivity of these assumptions with three additional scenarios. Particularly we consider the following cases (i) DSN3 plus the site in Santiago with the mask angles of 20° for DSN and of 6° for the lunar surface. (ii) DSN4 with the mask angles of 20° for DSN and of 6° for the lunar surface (iii) DSN3 plus the sites in Santiago and Hartebeesthoek with the mask angles of 20° for DSN and of 6° for the lunar surface. (iv) DSN3 with the mask angles of 0° for DSN and of 6° for the lunar surface. These results are detailed in Table 1; however, major points are emphasized here:

(a) Adding the Hartebeesthoek or the Santiago site to the primary DSN3 would increase the percentage of coverage, but would not extend the latitude of coverage

beyond ±76° latitudes. Nor does it help to greatly reduce the maximum gap times, especially in the polar regions.

(b) Due to its location, the Hartebeesthoek site compliments better with DSN3 than the Santiago site does in all aspects (coverage, gaps, number of gaps).

(c) When both the Hartebeesthoek and the Santiago sites are added to the primary DSN3, the near-side coverage percentage can increase to 97%. The number of gaps is reduced, but the maximum communication gaps still linger around 2.4 hours (same as DSN4 results).

(d) Lowering the DSN mask angle can maximize the percentage of coverage to 100% to the near-side equatorial region. As a result, the communication gaps in such regions can be wiped out.

(e) Future lunar manned missions to the polar regions might need more than just direct DSN support. Relay satellites around the Moon is a definite must.

| | | DSN3 (20° DSN Mask 6° Lunar Mask) | DSN3 + Santiago (20° DSN Mask 6° Lunar Mask) | DSN3 + Hartebeesthoek (20° DSN Mask 6° Lunar Mask) | DSN3 + Santiago & Hartebeesthoek (20° DSN Mask 6° Lunar Mask) | DSN3 (0° DSN Mask 6° Lunar Mask) |
|---|---|---|---|---|---|---|
| Single (%) | N | 13-87 | 13-91 | 13-95 | 13-97 | 16-100 |
| | Eq. | 87 | 91 | 95 | 97 | 100 |
| | S | Oct-87 | 16-91 | 16-95 | 16-97 | 13-100 |
| Max. Gap | N | 22 days | 22 days | 22 days | 22 days | 21.8 days |
| | Eq. | 3.6 hrs | 3.3 hrs | 2.4 hrs | 2.4 hrs | 0 hrs |
| | S | 13.6 days | 13.6 days | 13.6 days | 13.6 days | 13.6 days |
| No. of Gaps | N | 13-42 | 13-30 | 13-27 | 13-17 | 8-13 |
| | Eq. | 40+ | 30+ | 20+ | 16+ | 10+ |
| | S | 10-42 | 10-30 | 10-27 | 10-23 | 8-9 |
| Double (%) | N | 0-13 | 4-38 | 3-41 | 5-59 | 4-48 |
| | Eq. | 13 | 38 | 41 | 59 | 48 |
| | S | 1-13 | 4-38 | 2-41 | 6-59 | 4-48 |

Table 1: Coverage analysis for a few different DSN scenarios to the near-side lunar surface

## Constrained Optimization on the Lunar Communication Network

As indicated in the previous section, a network of lunar relay satellite is needed to provide better communication coverage of the Moon. In this section, we will investigate a few constellations of relay satellites around the Moon, each consists of six relay satellites in two planes. Our objective is to find a set of stable orbits that require very little trajectory maintenance. These constellations are designed to provide global coverage of the Moon and at the same time they are low in altitudes such that they can deliver telecom throughputs more efficiently and yield no communication gaps between relay satellites and the users on lunar surface. Our approach to this constrained optimization problem can be described as follows. Our goal is to find a constellation with the smallest possible the slanted range (thus more efficient data throughputs) such that the constellation is stable and provides 100% communication coverage. Since the simulation for coverage is very intensive, we will narrow our search space to the set of stable orbits. Thus let us start with simplified Lagrange Planetary Equations [2] for the third body perturbed problem,

$$\frac{de}{dt} = \frac{15}{8}\frac{n_M^2}{n_s} e\sqrt{1-e^2}\,\sin^2 i \sin 2\omega$$

$$\frac{di}{dt} = -\frac{15}{16}\frac{n_M^2}{n_s}\frac{e^2}{\sqrt{1-e^2}}\sin 2i \sin 2\omega$$

$$\frac{d\omega}{dt} = \frac{3}{8}\frac{n_M^2}{n_s}\frac{1}{\sqrt{1-e^2}}\left[5\cos^2 i - 1 + 5\sin^2 i \cos 2\omega + e^2(1-5\cos 2\omega)\right] + \frac{3n_s J_2}{2a^2(1-e^2)^2} e\cos i\left(1-\frac{5}{4}\sin^2 i\right)$$

where

$a$ ~ **semi major axis**

$e$ ~ **eccentricity**

$i$ ~ **inclination**

$\omega$ ~ **argument of perilune**

$$N_M = \sqrt{\frac{GM_E}{a_M^3}}$$

$$n_s = \sqrt{\frac{GM_M}{a_s^3}}$$

$G$ ~ **Universal Gravitational Constant**

$M_E$ ~ **Mass of Earth**

$M_M$ ~ **Mass of the Moon**

$J_2$ ~ **2nd Harmonic Gravity**

We next perform a trade study based on the orbit elements to determine the orbits of desire. Basically, we are looking for stable orbits that are librating around the line apsides with small changes in the orbital eccentricity and the inclination. Fixed point solutions to this system of ordinary differential equations (ODEs) can be found analytically. It can be easily verified that a stable solution would require the argument of Perilune to be 90° or 270°. To demonstrate the impacts of the eccentricity and the inclination angle on the stability of the orbit, we solve the above system of ODEs with a fixed orbital semi-major axis, as an for example of 5214 km, and the following initial conditions $\omega_0 = 90°$, $0 \le e_0 \le 0.95$, and $0° \le i_0 \le 180°$ for 100 years. We then take the resulting temporal profiles of the eccentricity, inclination, and argument of Perilune and calculate the maximum variations $[\Delta e, \Delta i, \Delta\omega]$. To represent the stability with a single metric, we compute the following heuristic cost function for each initial value

$$J(e_0, i_0) = \frac{F(\Delta e)}{1} + \frac{F(2\pi\Delta\omega)}{10} + \frac{F(\pi\Delta i)}{100}$$

where,

$$F(X) = (X > 0.1) * \frac{floor(X * 10)}{10}$$

It should be noted from $F(X)$ that whenever the maximum variation exceeds 10%, the cost function would substantiate. Weights are also added to the cost function with more emphasis on the eccentricity and argument of Perilune than the inclination. This cost function is in some sense normalized and varies between 0 and 1. Its tenth, hundredth, and thousandth decimal places represent the variations in the eccentricity, argument of Perilune and inclination respectively. The plot for the cost function over the entire trade space of eccentricity and inclination is displayed in Figure 5. The area for which the cost function is minimal (designated in red asterisks) include

(i) $e_0 = 0$ with $I_0 \le i_0 \le 180° - I_0$,

(ii) $e_0^2 = \cos(i_0 - 90° / I_0 - 90°)$

where $I_0 = 39.2°$ is the critical inclination in the 3rd body perturbation problem.

The previous results allow us to pinpoint where in the trade space (eccentricity and inclination with fixed semi-major axis and argument of Perilune) the set of orbits that are stable. Our next step is to investigate their coverage performance and thus we select a set of seven stable orbits for further communication coverage analysis. Different combinations of stable eccentricities with prograde, retrograde and critically inclined inclinations are shown in Table 2. These orbits are simulated for 100 years and the results $(e(t), \omega(t))$ are displayed in Figure 6. It can be seen that while the elliptical orbits are librating, the eccentricities of the two circular orbits remain zero.

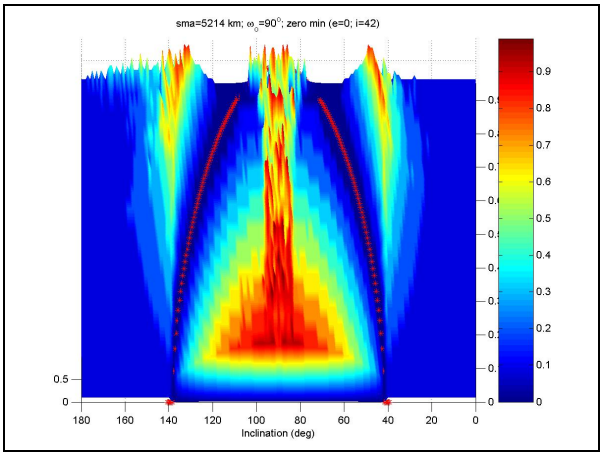


Fig. 5: 100-year stability cost function over the trade space of eccentricity and inclination (**a** and **ω** are kept at 5214km and 90°, respectively)

| Orbit | Eccentricity | Inclination |
|---|---|---|
| 1 | 0.00 | 63.43 |
| 2 | 0.00 | 138.46 |
| 3 | 0.15 | 43.50 |
| 4 | 0.20 | 138.00 |
| 5 | 0.25 | 45.00 |
| 6 | 0.30 | 136.50 |
| 7 | 0.35 | 47.00 |

Table 2: Initial conditions for a set of selected stable orbits (**a** and **ω** are kept at 5214km and 90°, respectively)

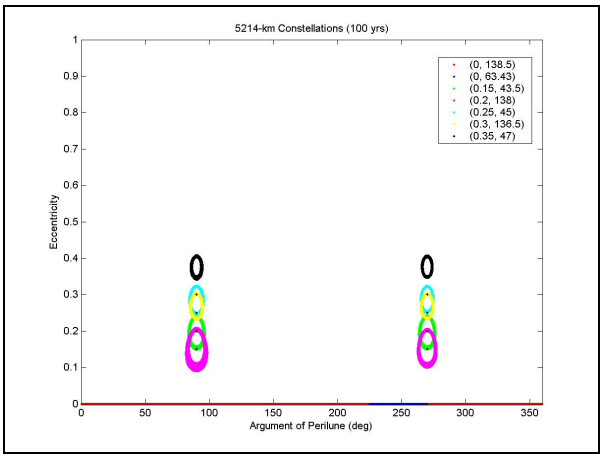


Fig. 6: Eccentricities versus the inclination angles for the selected orbits over 100 years

For each of the above orbit, we form its corresponding constellation in the following manner. The semi-major axis is fixed at 5214 km, the eccentricity and inclination angle are taken from the selected list. The remaining orbital elements for each constellation are displayed in Table 3.

| Orbiter | Ascending Node | Argument of Perilune | Mean Anomaly |
|---|---|---|---|
| 1 | 90 | 90 | 0 |
| 2 | 90 | 90 | 120 |
| 3 | 90 | 90 | 240 |
| 4 | 180 | 270 | 0 |
| 5 | 180 | 270 | 120 |
| 6 | 180 | 270 | 240 |

Table 3: The remaining orbital element for the six constellations (the semi-major is kept at 5214 km and the eccentricity and inclination are in Table 2)

For each constellation, we propagate for one lunar sidereal month the trajectories for the orbiters. Then for each longitude/latitude point on the lunar surface we calculate its view period with the orbiters of the constellation using 0° elevation mask angle. As a result, we can compute the percentage of coverage by the constellation for the entire lunar surface. The worst (min), area-weighted average (A-W mean) and the best (max) visibility information for the six 5214-km constellations is recorded in Table 4.

| Visibility Percentage (0° Lunar Elevation Mask) | | | |
|---|---|---|---|
| Constellation | Min | A-W Mean | Max |
| 1 | 100 | 100 | 100 |
| 2 | 98.09 | 99.83 | 100 |
| 3 | 97.39 | 99.45 | 100 |
| 4 | 89.44 | 98.96 | 100 |
| 5 | 95.16 | 98.68 | 100 |
| 6 | 88.25 | 98.14 | 100 |
| 7 | 93.52 | 97.78 | 100 |

Table 4: Visibility for the six 5214-km constellations

Some important observations can be found from Table 4. First with this configuration of the constellations, circular orbits provide better communication coverage than those that are elliptical. The same thing can be said for the prograde orbiters. Most importantly is the fact that all of these constellations can achieve 100% visibility. Incidently, we have found that the semi-major axis of 5214 km is the lowest value for which the constellation can provide 100% visibility to the entire lunar surface with 0° elevation mask angle.

Based on the visibility analysis found for the 5214-km constellation, we have come up with another critically inclined constellation, which with a 7278-km semi-major axis (sma) can provide 100% global coverage (i.e. 6° elevation mask angle). From now on, we refer to both of these circular critically inclined orbits as CCI-5214 and CCI-7278. It should be remarked here that these constellations are stable under the Lagrange Planetary Equations. In the full nonlinear regime, some minor station keeping may be needed from time to time.

For comparing purposes we also consider two elliptical constellations proposed by [1]. The orbital elements for these final four lunar constellations are given in Tables 3 and 5.

| Constellation | sma (km) | eccentricity | inclination |
|---|---|---|---|
| A | 7500 | 0.050 | 40.0000 |
| B | 9873 | 0.185 | 40.0000 |
| CCI-5214 | 5214 | 0.000 | 63.4349 |
| CCI-7278 | 7278 | 0.000 | 63.4349 |

Table 5: Partial orbital elements for the final four constellations

Using the orbital element in Table 5 as initial conditions we propagate the above system of ODEs for 100 years and examine the dynamics of the eccentricities and the arguments of Perilune in Figure 7 to ensure that these constellations are stable.

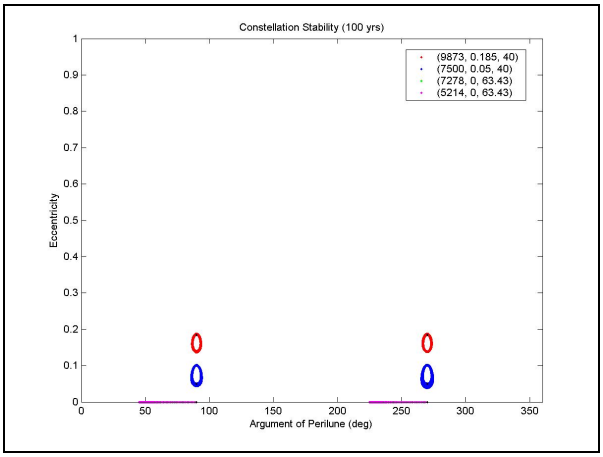


Fig. 7: 100-year dynamics of the eccentricities versus the arguments of Perilune for the final four constellations

We next compare the performances of these final four constellations. In Figure 8, we show

the percentage of visibility (0° lunar elevation mask) based on one lunar sidereal month. All four constellations perform well in the single visibility category. Only in a few locations on the lunar surface, single visibility to Constellation A is at 99.5%. Perfection can be done with a small adjustment in the semi-major axis. The rest of the constellations can all achieve 100% visibility. In the double and triple visibility categories, as expected due to their higher semi-major axis, both the Constellation B and Constellation CCI-7278 perform comparably well and better than the remaining two constellations.

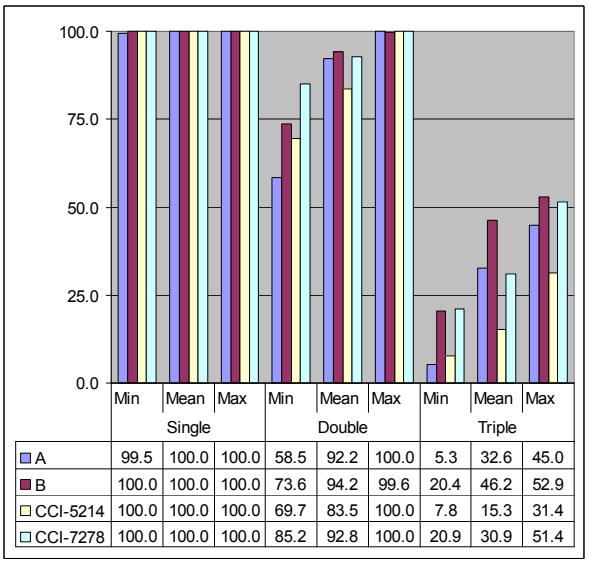


| | Single | | | Double | | | Triple | | |
|---|---|---|---|---|---|---|---|---|---|
| | Min | Mean | Max | Min | Mean | Max | Min | Mean | Max |
| A | 99.5 | 100.0 | 100.0 | 58.5 | 92.2 | 100.0 | 5.3 | 32.6 | 45.0 |
| B | 100.0 | 100.0 | 100.0 | 73.6 | 94.2 | 99.6 | 20.4 | 46.2 | 52.9 |
| CCI-5214 | 100.0 | 100.0 | 100.0 | 69.7 | 83.5 | 100.0 | 7.8 | 15.3 | 31.4 |
| CCI-7278 | 100.0 | 100.0 | 100.0 | 85.2 | 92.8 | 100.0 | 20.9 | 30.9 | 51.4 |

Fig. 8: Single, double and triple visibility percentages for the considered constellations (0° lunar elevation mask)

Table 6 show the visibility gap information for the four considered constellations. The optimized constellations truly met the 100% visibility constraint and thus produce no gaps.

| Visibility | Gaps (minutes) | | | No. of Gaps | | |
|---|---|---|---|---|---|---|
| Constellation | Min | Mean | Max | Min | Mean | Max |
| A | 0.0 | 8.7 | 74.8 | 0.0 | 1.1 | 13.0 |
| B | 0.0 | 0.8 | 7.9 | 0.0 | 0.1 | 2.0 |
| CCI-5214 | 0.0 | 0.0 | 0.0 | 0.0 | 0.0 | 0.0 |
| CCI-7278 | 0.0 | 0.0 | 0.0 | 0.0 | 0.0 | 0.0 |

Table 6: Maximum visibility gaps for the considered constellations (0° lunar elevation mask)

Let us now address the communication coverage of these considered constellations. That is to examine their performance with the 6° lunar elevation mask. The single, double and triple coverage percentages are detailed in Figure 9 and the communication gaps information is displayed in Table 7. Keep in mind that Constellations A, B, and CCI-5214 are designed to achieve the 100% visibility, whereas the Constellation CCI-7278 were optimized for 100% coverage. However they all perform remarkably well as their area-weighted averages for the single coverage percentages are 99.5% or more. As expected, due to the 100% coverage constraint, the optimized Constellation CCI-7278 experiences no communication gaps with any users on the lunar surface. We also provide the communication gap information for the other constellations with the understanding that they do not belong to the same design.

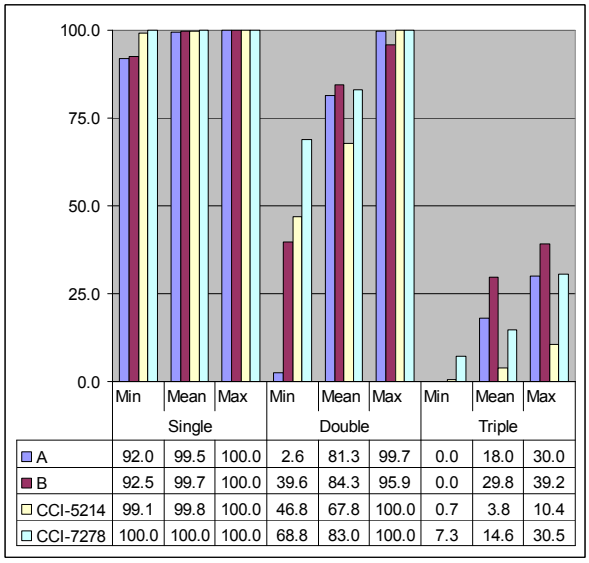


| | Single | | | Double | | | Triple | | |
|---|---|---|---|---|---|---|---|---|---|
| | Min | Mean | Max | Min | Mean | Max | Min | Mean | Max |
| A | 92.0 | 99.5 | 100.0 | 2.6 | 81.3 | 99.7 | 0.0 | 18.0 | 30.0 |
| B | 92.5 | 99.7 | 100.0 | 39.6 | 84.3 | 95.9 | 0.0 | 29.8 | 39.2 |
| CCI-5214 | 99.1 | 99.8 | 100.0 | 46.8 | 67.8 | 100.0 | 0.7 | 3.8 | 10.4 |
| CCI-7278 | 100.0 | 100.0 | 100.0 | 68.8 | 83.0 | 100.0 | 7.3 | 14.6 | 30.5 |

Fig. 9: Single, double and triple coverage percentages for the considered constellations (6° lunar elevation mask)

| Coverage | Gaps (minutes) | | | No. of Gaps | | |
|---|---|---|---|---|---|---|
| Constellation | Min | Mean | Max | Min | Mean | Max |
| A | 0.0 | 34.5 | 149.5 | 0.0 | 9.4 | 94.0 |
| B | 0.0 | 48.6 | 102.3 | 0.0 | 10.7 | 80.0 |
| CCI-5214 | 0.0 | 18.4 | 35.4 | 0.0 | 13.8 | 30.0 |
| CCI-7278 | 0.0 | 0.0 | 0.0 | 0.0 | 0.0 | 0.0 |

Table 7: Maximum coverage gaps for the considered constellations (6° lunar elevation mask)

## Lunar Surface and DSN Connectivity

We now address the communication coverage between the DSN stations and locations on the lunar surface. As seen in Figure 1, the lunar Polar Regions, the near-side borders and the far-side areas receive little or no coverage. The relay service provided by the constellation of orbiters can fill such extension. Figure 10 shows the global map of communication coverage

percentages of a lunar location to DSN3 via either a direct link or relay through the Constellation B. It can be noticed from the Figures that with the relay constellation those regions which receive little or no coverage by the DSN stations can now enjoy almost the same percentages as if they were on the near side. Here we assume the elevation mask angle for DSN is 20° and for the lunar surface is 6°. The latitude map of these coverage percentages in Figure 11 tells us that any point on the lunar surface will have from 82% to 88% of the time connection to one of the DSN3 stations either via a direct link or relay link through an orbiter of the Constellation B.

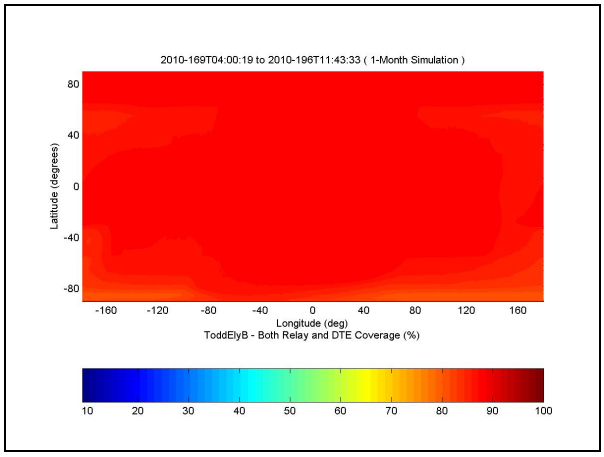


Fig. 10: Global map of connectivity percentages between a lunar surface location and the DSN via either direct or relay link through Constellation B to DSN3. (20° DSN and 6° lunar elevation masks)

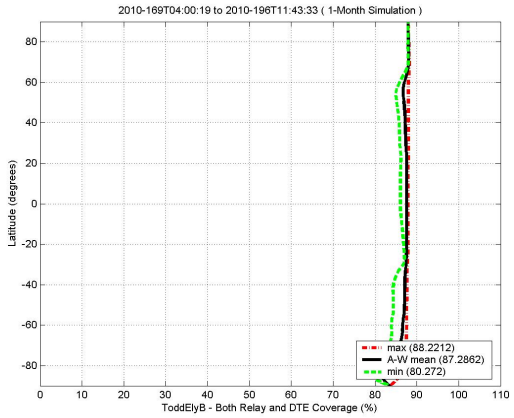


Fig. 11: Latitude map of connectivity percentages between a lunar surface location and the DSN via either direct or relay link through Constellation B to DSN3. (20° DSN and 6° lunar elevation masks)

It can be seen from Figure 12 that the connectivity between the DSN and the lunar far side can be improved significantly via the relay orbiters. On the average, 86% of the time or more a point on the lunar surface can connect to one of the DSN3 stations. Such communication coverage percentage can increase to 90% when Hartebeesthoek is added to the DSN3 or almost 100% if the elevation mask angle for the DSN stations is lowered to 0°.

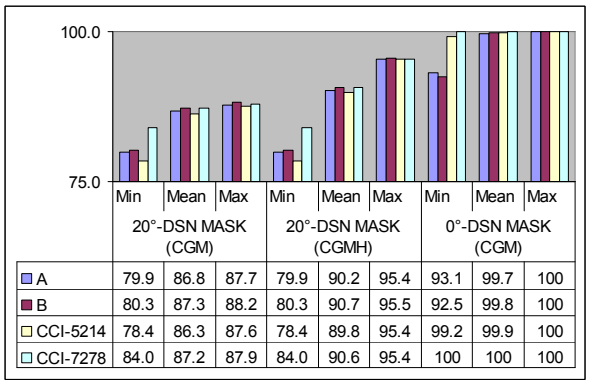


| | 20°-DSN MASK (CGM) | | | 20°-DSN MASK (CGMH) | | | 0°-DSN MASK (CGM) | | |
|---|---|---|---|---|---|---|---|---|---|
| | Min | Mean | Max | Min | Mean | Max | Min | Mean | Max |
| A | 79.9 | 86.8 | 87.7 | 79.9 | 90.2 | 95.4 | 93.1 | 99.7 | 100 |
| B | 80.3 | 87.3 | 88.2 | 80.3 | 90.7 | 95.5 | 92.5 | 99.8 | 100 |
| CCI-5214 | 78.4 | 86.3 | 87.6 | 78.4 | 89.8 | 95.4 | 99.2 | 99.9 | 100 |
| CCI-7278 | 84.0 | 87.2 | 87.9 | 84.0 | 90.6 | 95.4 | 100 | 100 | 100 |

Fig. 12: Connectivity percentages between a lunar surface location and the DSN via direct or relay link. (6° lunar elevation mask; DSN sites include Canberra, Goldstone, Madrid and Hartebeesthoek)

The gaps information for the DSN connectivity can be found in Figures 13-14. The maximum gaps are between 3-5 hours. Adding the Hartebeesthoek site will reduce both the maximum gap time and the number of gaps on the near-side region.

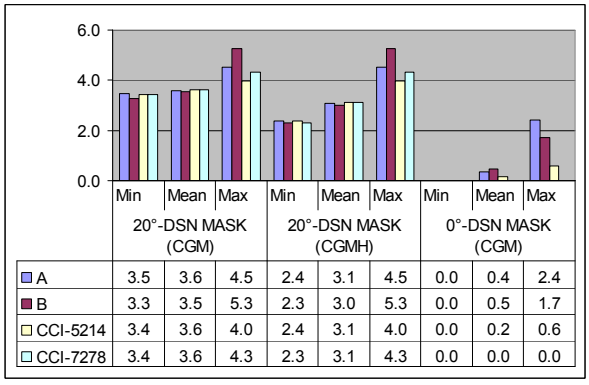


| | 20°-DSN MASK (CGM) | | | 20°-DSN MASK (CGMH) | | | 0°-DSN MASK (CGM) | | |
|---|---|---|---|---|---|---|---|---|---|
| | Min | Mean | Max | Min | Mean | Max | Min | Mean | Max |
| A | 3.5 | 3.6 | 4.5 | 2.4 | 3.1 | 4.5 | 0.0 | 0.4 | 2.4 |
| B | 3.3 | 3.5 | 5.3 | 2.3 | 3.0 | 5.3 | 0.0 | 0.5 | 1.7 |
| CCI-5214 | 3.4 | 3.6 | 4.0 | 2.4 | 3.1 | 4.0 | 0.0 | 0.2 | 0.6 |
| CCI-7278 | 3.4 | 3.6 | 4.3 | 2.3 | 3.1 | 4.3 | 0.0 | 0.0 | 0.0 |

Fig. 13: Maximum connectivity gaps (hrs) between a lunar surface location and the DSN via direct or relay link. (6° lunar elevation mask; DSN sites include Canberra, Goldstone, Madrid and Hartebeesthoek)

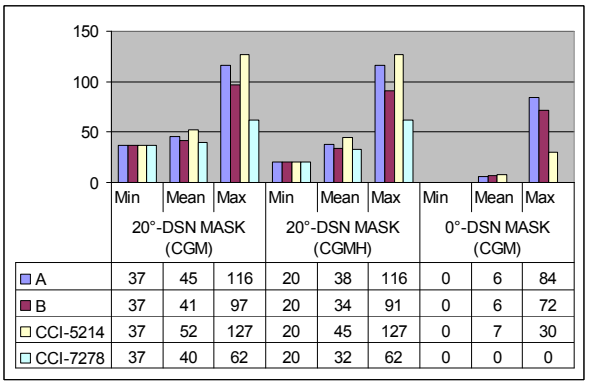


| | Min | Mean | Max | Min | Mean | Max | Min | Mean | Max |
|---|---|---|---|---|---|---|---|---|---|
| | 20°-DSN MASK (CGM) | | | 20°-DSN MASK (CGMH) | | | 0°-DSN MASK (CGM) | | |
| A | 37 | 45 | 116 | 20 | 38 | 116 | 0 | 6 | 84 |
| B | 37 | 41 | 97 | 20 | 34 | 91 | 0 | 6 | 72 |
| CCI-5214 | 37 | 52 | 127 | 20 | 45 | 127 | 0 | 7 | 30 |
| CCI-7278 | 37 | 40 | 62 | 20 | 32 | 62 | 0 | 0 | 0 |

Fig. 14: Number of connectivity gaps between a lunar surface location and the DSN via direct or relay link. (DSN sites include Canberra, Goldstone, Madrid and Hartebeesthoek)

### Crosslink Necessity

The results in Figure 12-14 show that continuous communication between a point on the lunar surface and one of the DSN stations is not achievable with 20° DSN elevation mask angle. A natural suggestion would be to equip the relay orbiters with the crosslink capability so that if an orbiter which does not have a direct link with a DSN station but is in view with a user on the surface can relay the information to another orbiter that has direct link with a DSN station. If we compare the communication gaps between the DSN stations and the near-side region in Table 1, we can see that even points on the near side experience forty or more gaps and some of them could be as long as 3.6 hours. Thus adding the crosslink capability only reduce the upper bounds on the maximum communication gaps (5 hours down to 3.6 hours), but will not provide continuous communication between any location on the lunar surface with the DSN stations. Information in Figures 12-14 also indicates that if the mask angle for DSN is reduced to 0°, continuous communication between the DSN stations and the points on the lunar surface is possible with the Constellation CCI-7278. Another suggestion would be to tap into a network of Earth relay satellites such as Telemetry Data Relay Satellite System (TDRSS).

### Relay Latency and its Mitigations

Communication between a point on the lunar surface directly to DSN or direct bent pipe via a relay satellite will experience some gaps (3-5 hours) shown in Figure 13. However at such instances, any point on the lunar surface can have continuous communication at least to the Constellation CCI-7278. Thus a point on the lunar far side might have to wait more than 5 hours to have a direct communication with one of the DSN stations. By going through the store-and-forward mode, such communication gap can possibly be reduced to the level comparable to the occulting time due to the Moon. The worst case scenario occulting times for the considered constellations are displayed in Table 8 along with the information on the furthest slanted range and the altitudes of the Perilune of the four considered constellations. It should be noticed that these ranges can directly impact on the occulting time as well as the communication efficiency.

| Constellation | Furthest Slanted Range (km) | Perilune Altitude (km) | Max Occulting Period (minutes) |
|---|---|---|---|
| A | 7501 | 5387 | 73.8 |
| B | 11389 | 6308 | 84.9 |
| CCI-5214 | 4737 | 3476 | 61.8 |
| CCI-7278 | 6888 | 5540 | 72.7 |

Table 8: Constellation minimum and maximum ranges and the maximum occulting time due to the Moon

### Conclusions

A number of important findings can be extracted from this article. The primary Goldstone, Canberra, Madrid (DSN3) sites of the Deep Space Network along with potential stations at Hartebeesthoek, South Africa and Santiago, Chile cannot provide continuous coverage to the lunar surface, even at locations on the near side of the Moon. Such limitation is caused mainly by the assumed 20° DSN elevation mask angle. Nevertheless, under such assumption along with the 6° lunar elevation mask angle, the near-side coverage is 87% for DSN3, 91% for DSN3 plus Santiago, 95% for DSN3 plus Hartebeesthoek, and 97% for DSN3 plus both Santiago and Hartebeesthoek. Continuous coverage of the near side is possible when the 20° DSN elevation mask angle condition is removed. As from the second part of the paper, two set of stable constellations are found from our constrained optimization scheme. Both are optimized in the sense that they are stable and they are the lowest (thus most efficient in delivering data throughputs) to provide 100% visibility and 100% communication coverage. Other metrics such as the maximum and the

number of communication gaps are also computed. With the 20° DSN 6° lunar elevation mask angle assumptions, we found that our optimized constellation can connect any users on the lunar surface to the DSN3 87%, to DSN3 plus Hartebeesthoek 91% and remarkably 100% if the DSN mask angle condition is nullified. Finally, the maximum communication gap to DSN3 can be 3.6 hours on the near-side and 4.3 hours in the far side of the Moon. Since locations on the near side of the Moon also suffer communication gaps, the orbiter-to-orbiter crosslink capability cannot make the 4.3 hours of gap time vanished for the far-side lunar location. Finally, one way to mitigate such gap is to implement the store-and-forward capability. By planning carefully, a user on the lunar surface can send data to an orbiter and have it send to the DSN stations when it exits its occultation period. The worst case scenario occulting time for the constellations is between 1 to 1.5 hours. Another suggestion would be to have the lunar constellation communicate to a network of Earth relay satellites such as Telemetry Data Relay Satellite System (TDRSS).

## References

[1] Ely, Todd A. and Lieb Erica, "*Constellations of elliptical inclined lunar orbits providing polar and global coverage*," Proceedings of the AAS/AIAA Astrodynamics Specialists Conference, AAS-05-343, Lake Tahoe, CA, 2005

[2] Chobotov, V., Editor, *Orbital Mechanics, Second Edition*, American Institute of Astronautics, Inc., Reston, VA, 1996

## Acknowledgements

The authors wish to thank Dr. Todd A. Ely for the information on the lunar constellations and their stability. The research in this paper was carried out in part at the Jet Propulsion Laboratory at California Institute of Technology, under a contract with the National Aeronautics and Space Administration and at the Department of Mathematics at the California State University Fullerton.